# Journal of Materials Chemistry B

Accepted Manuscript






ROYAL SOCIETY OF CHEMISTRY

www.rsc.org/materialsB

Cite this: DOI: 10.1039/c0xx00000x

www.rsc.org/xxxxxx

**Full Paper**

# Self-polymerization of Dopamine and Polyethyleneimine: Novel Fluorescent Organic Nanoprobes for Biological Imaging Applications

**Meiying Liu [a,c], Jinzhao Ji[b], Xiaoyong Zhang[a, b,*], Xiqi Zhang[b], Bin Yang[b], Fengjie Deng[a], Zhen Li[b], Ke Wang[b], Yang Yang[b], Yen Wei[b,*]**

*Received (in XXX, XXX) Xth XXXXXXXXX 20XX, Accepted Xth XXXXXXXXX 20XX*
**DOI: 10.1039/b000000x**

**The development of novel fluorescent nanoprobes has attracted great current research interest over the past few decades due to their superior optical properties and multifunctional capability as compared with small organic dyes. Although great advance has been made in utilization of fluorescent nanoprobes for biomedical applications, development of novel fluorescent nanoprobes that possess good fluorescent properties, biocompatibility, biodegradability and water dispersibility through a convenient and effective route is still highly desirable. In this work, we reported for the first time that novel fluorescent organic nanoparticles (FONs) can be conveniently fabricated via self-polymerization of dopamine and polyethyleneimine under room temperature and air atmosphere within 2 h. These FONs exhibited strong green fluorescence, high water stability and excellent biocompatibility, making them highly potential for biological imaging applications. More importantly, due to the high reactive of polydopamine, these FONs might also be further functionalized with other functional components through Michael addition or Schiff base reaction. Therefore the method described in this work would open new avenues for fabrication of fluorescent nanoprobes for various biomedical applications.**

## 1. Introduction

Since the first utilization of semiconductor quantum dots as biological lables in 1998, a number of fluorescent nanoparticles have been fabricated and considered for bioimaging applications.[1-4] Based on their compositions, these fluorescent nanoparticles can be mainly divided into fluorescent inorganic nanoparticles (FINs) and fluorescent organic nanoparticles (FONs).[5-9] As a promising nanoprobe, it should be of suitable size and size distribution, high water dispersibility, good biocompatibility and biodegradability. Although FINs possess remarkable fluorescent properties and have been widely explored for bioimaging applications, most of FINs are non-biodegredable and some of them have demonstrated to be toxic to living organisms.[10] Therefore, the searching of alternative nanoprobes, which could overcome the problems of FINs is still of great research interest.

Because of their advantages such as biodegradable potential, designability, surface chemistry tailorability and biocompatibility, FONs have been regarded as the promising candidates for bioimaging applications.[11-15] A variety of FONs based on small organic dyes, conjugate polymers and aggregation induced emission (AIE) dyes have been reported over the past few decades.[16-20] A general strategy for fabrication of FONs is incorporation of hydrophobic dyes into hydrophilic polymers, thus forming of dyes contained amphiphilic copolymers. These amphiphilic copolymers can be self assembled into FONs in aqueous solution, in which hydrophobic dyes were encapsulated in the core of FONs and hydrophilic polymers were covered on the surface of hydrophobic core to render them water dispersibility. Although significant progress has been made, it still has some problems for preparation of highly luminescent FONs based on conventional organic dyes because of the aggregation-caused quenching (ACQ) effect.[21] It is well known that the fluorescence of conventional organic dyes will be quenched severely in their solid and aggregation state. Decrease the concentrations of dyes could ease up the quenching effect, however, it is still difficult to obtain ultrabright FONs because of the limited fluorescent chromophores. FONs based on AIE dyes could avoid the ACQ effect, however, the synthesis of AIE dyes and preparation of AIE dye based FONs are rather complex and time-consuming.[22, 23] Therefore, the preparation of highly luminescent FONs with good water dispersibility and excellent biocompatibility through a rather simple method is highly desirable.

Dopamine (DA) is a neurotransmitter in the catecholamine and phenethylamine families that plays an important role in the brains and bodies of living organisms. It has also been reported that DA could be self-polymerized in alkaline solution to form polydopamine (PDA), which can be deposited on virtually all types of surface.[24] Since the first report of mussel inspired chemistry for surface modification, mussel inspired chemistry has been widely explored for different applications ranged from energy storage and conversion to environment remedation and biomedicine.[24-39] Especially, various nanostructures based on PDA with distinct size and properties have recently been fabricated and explored

for biomedical applications.[40] For example, Lu *et al* have reported that colloid PDA nanospheres with tunable size can be used as novel photothermal therapeutic agents for *in vivo* cancer therapy. The photothermal conversion efficiency of these PDA nanospheres is as high as 40%, which is much higher than that of Au nanorods.[41] On the other hand, the preparation of nitrogen doped fluorescent carbon nanodots using DA as the carbon and nitrogen sources was recently reported by Qu et al. They demonstrated that these carbon dots with size of about 3.8 nm and excitation dependent photoluminescent can be obtained through one-step hydrothermal treatment. And these carbon dots can be used for seletive determination of $Fe^{3+}$ in solution and for living cell imaging.[42] More recently. the preparation of PDA FONs through oxidation of PDA with concentrated $H_2O_2$ was developed by our group.[43] We demonstrated that PDA FONs with strong fluorescence and excellent biocompatibility were promising for bioimaging applications. This study open up a new orientation for preparation of FONs via mussel inspired chemistry. However, the disadvantages of these above methods are time consuming, requirement of hazardous agent ($H_2O_2$) and high reaction temperature.

In this contribution, we reported a rather convenient and effective strategy for preparation of PDA based FONs through self-polymerization of DA in the present of polyethyleneimine (PEI) for the first time (Fig. 1). In this reaction system, PEI could provide the alkaline environment which promoted polymerization of DA. On the other hand, PEI could also react with DA through Michael addition reaction. Various techniques such as fluorescence spectroscopy, transmission electron microscope (TEM), Fourier transform infrared spectroscopy (FT-IR) and X-ray photoelectron spectroscopy (XPS) have been used to characterize **PEI-PDA** FONs. To explore their biomedical application potential, the cell uptake behavior of **PEI-PDA** FONs was also visualized.

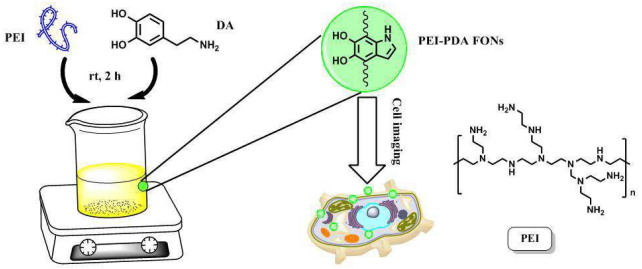


**Fig. 1** Schematic showing the preparation of **PEI-PDA** FONs through self-polymerization using polyetheniemine (PEI) and dopamine (DA) as the precursors and cell imaging applications of **PEI-PDA** FONs.

## 2. Materials and methods

### 2.1 Materials and measurements

Polyethyleneimine (PEI, Mn = 600, alading reagent Inc. Shanghai, China), DA (Sangon biotech, Shanghai, China) were used as received. All other solvents and chemicals were purchased from commercial sources and used directly without further purification. Fluorescence spectra were measured on a PE LS-55 spectrometer with a slit width of 3 nm for both excitation and emission. The FT-IR spectra were obtained in a transmission mode on a Perkin-Elmer Spectrum 100 spectrometer (Waltham, MA, USA). Typically, 8 scans at a resolution of 1 $cm^{-1}$ were accumulated to obtain one spectrum. Transmission electron microscopy (TEM) images were recorded on a JEM-1200EX microscope operated at 100 kV, the TEM specimens were made by placing a drop of the nanoparticle suspension on a carbon-coated copper grid. The hydrodynamic size distribution of **PEI-PDA** FONs in water and phosphate buffer solution (PBS) was determined using a zeta Plus apparatus (ZetaPlus, Brookhaven Instruments, Holtsville, NY). The XPS was performed on a VGESCALAB 220-IXL spectrometer using an Al Kα X-ray source (1486.6 eV). The energy scale was internally calibrated by referencing to the binding energy (Eb) of the C1s peak of a carbon contaminant at 284.6 eV.

### 2.2 Preparation of PEI-PDA FONs

PEI (100 mg) and DA (200 mg) was dispersed in 20 mL deionized water for 2 h at room temperature. Then the mixture was purified by dialysis through porous cellulose bag (molecular weight cut off 3500 Da) using absolutely ethanol for 24 h. Finally the products inside the dialysis bag were collected and dried by vacuum oven at 40 °C for 24 h.

### 2.3 Cytotoxicity of PEI-PDA FONs

Cell morphology was examined to evaluate the effects of **PEI-PDA** FONs to human lung adenocarcinoma epithelial (A549) cells. Briefly, cells were seeded in 6-well microplates at a density of $1\times10^5$ cells $mL^{-1}$ in 2 mL of Dulbecco's modified eagle medium (DMEM) cell culture medium containing 10% fetal bovine serum (FBS). After 24 h of cell attachment, plates were washed with PBS and cells were treated with DMEM cell culture medium, or different concentrations of **PEI-PDA** FONs prepared in 10% FBS containing media for 24 h. Then all samples were washed with PBS three times to remove the uninternalized nanoparticles. The morphology of cells was observed by using an optical microscopy (Leica, Germany), the overall magnification was × 100.

The cell viability of **PEI-PDA** FONs on A549 cells was evaluated by cell counting kit-8 (CCK-8) assay based on our previous reports.[44] Briefly, cells were seeded in 96-well microplates at a density of $5\times10^4$ cells $mL^{-1}$ in 160 μL of respective media containing 10% FBS. After 24 h of cell attachment, the cells were incubated with 10, 20, 40, 80, 120 μg $mL^{-1}$ **PEI-PDA** FONs for 8 and 24 h. Then nanoparticles were removed and cells were washed with PBS three times. 10 μL of CCK-8 dye and 100 μL of DMEM cell culture medium were added to each well and incubated for 2 h at 37 °C. Plates were then analyzed with a microplate reader (VictorIII, Perkin-Elmer). Measurements of formazan dye absorbance were carried out at 450 nm, with the reference wavelength at 620 nm. The values were proportional to the number of live cells. The percent reduction of CCK-8 dye was compared to controls (cells not exposure to **PEI-PDA** FONs), which represented 100% CCK-8 reduction. Three replicate wells were used per microplate, and the experiment was repeated three times. Cell survival was expressed as absorbance

relative to that of untreated controls. Results are presented as mean ± standard deviation (SD).

### 2.4 Confocal microscopic imaging of cells using PEI-PDA FONs

A549 cells were cultured in DMEM supplemented with 10% heat-inactivated FBS, 2 mM glutamine, 100 U $mL^{-1}$ penicillin, and 100 μg $mL^{-1}$ of streptomycin. Cell culture was maintained at 37 °C in a humidified condition of 95% air and 5% $CO_2$ in culture medium. Culture medium was changed every three days for maintaining the exponential growth of the cells. On the day prior to treatment, cells were seeded in a glass bottom dish with a density of $1\times10^5$ cells per dish with size φ20 mm. On the day of treatment, the cells were incubated with **PEI-PDA** FONs at a final concentration of 10 μg $mL^{-1}$ for 3 h at 37 °C. Afterward, the cells were washed three times with PBS to remove the **PEI-PDA** FONs and then fixed with 4% paraformaldehyde for 10 min at room temperature. Cell images were taken with a confocal laser scanning microscope (CLSM) Zesis 710 3-channel (Zesis, Germany) with the excitation wavelength of 405 and 458 nm.

## 3 Results and discussion

### 3.1 Characterization of PEI-PDA FONs

Fig. 2 showed the TEM images of **PEI-PDA** FONs, many amphorous nanoparticles was observed (Fig. 2A), evidencing the successful formation of **PEI-PDA** FONs through the rather facile method. As confirmed by the high magnification TEM, the diameter of PEI-PDA FONs is about 100 nm (Fig. 2B). Significant different from the typical core-shell polymer nanoparticles, the **PEI-PDA** FONs are not standard spherical. Many nanoplates with tens of nanometers in diameter stack into spherical nanoparticles can also be distinguished by TEM observation. The possible force for formation of **PEI-PDA** FONs might be ascribed to π-π interaction between PDA and cross-linkage of PDA by PEI, which was formed by self-polymerization of DA in the present of PEI. On the other hand, we believed that **PEI-PDA** FONs were stable in aqueous solution due to PDA could be cross-linked by PEI through Michael addition reaction.[45, 46] The hydrodynamic size of **PEI-PDA** FONs in water and PBS was also determined by dynamic laser scattering (DLS). Results show that the size of **PEI-PDA** FONs in water is 159.8 ± 65.7 nm with polydispersity index (PDI) of 0.288 (Fig. S1A). When **PEI-PDA** FONs were dispersed in PBS, their size was increased to 213.4 ± 85.1 with PDI of 0.252 (Fig. S1B).

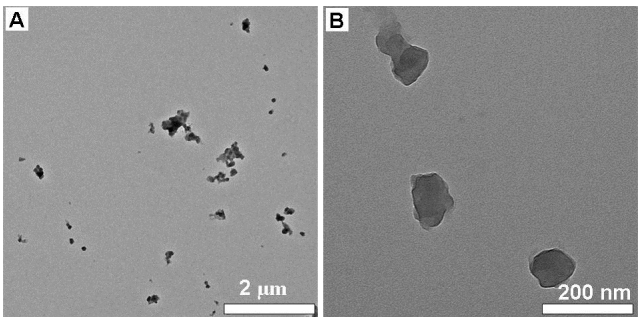


**Fig. 2** TEM images of **PEI-PDA** FONs with different magnificant, scale bar = 2 μm (A), and 200 nm (B).

Fig. 3 showed the IR spectra of **DA** and **PEI-PDA**. A series of absorbance bands located between 1450-1600 $cm^{-1}$ in **DA** were identified from the IR spectra, which are possibly ascribed to the stretching vibration of polycyclic aromatic rings of **DA**. The absorption peak at 1285 $cm^{-1}$ assigned to stretching vibration of phenolic C-O was also found in the spectrum of DA. On the other hand, two peaks at 2954 and 3035 $cm^{-1}$ with strong absorbance intensity were observed in spectrum of DA. These absorbance signals could be attributed to the stretching vibration of C-H bond. As compared with DA, the absorption of aminate I located at 1654 $cm^{-1}$ was significantly enhanced in **PEI-PDA** FONs. While the intensity of polycyclic aromatic rings was decreased correspondingly. These results suggested that the PEI has indeed incorporated with PDA. And **PEI-PDA** FONs have been successfully prepared via self-polymerization of DA and PEI. It is well known that DA could self-polymerized under alkaline solution. In the reaction system, the PEI could provide an alkaline environment, which promote the polymerization of DA in aqueous solution. On the other hand, the $NH_2$ group in PEI could also reacted with DA through Michael addition with aromatic rings or formation of imine with phenolic hydroxyl through Schiff base reaction.

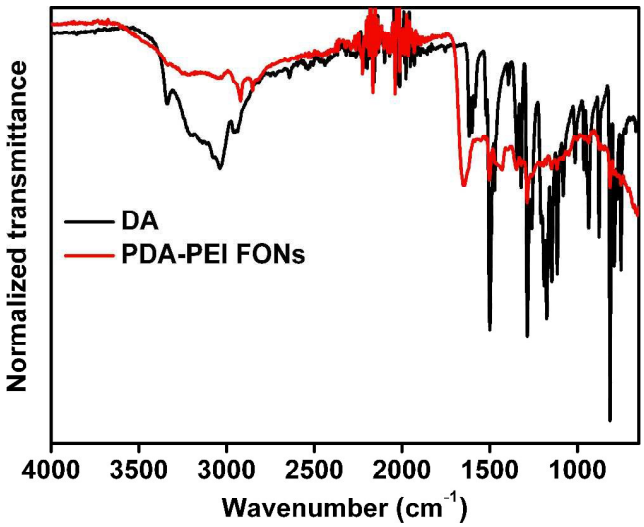


**Fig. 3** FT-IR spectra of DA and **PEI-PDA** FONs.

The chemical compositions of **PEI-PDA** FONs were characterized by XPS. It can be seen that the elements such as carbon (C), nitrogen (N) and oxygen (O) were existed in the samples of **PEI-PDA** FONs (Fig. 4A). The binding energy peaks of C, N, O were located at 284.8, 398.3 and 531.4 eV respectively (Fig. 4B-D). According to the XPS spectra, the percentages of C, N and O in the sample of **PEI-PDA** FONs are 77.9%, 15.2% and 6.9%, respectively. As compared with the DA, the percentage of N was significantly increased from 9.1% to 15.2%. However, the percentage of O was decreased from 20.9% to 6.9%. These results further confirmed that PEI was incorporated into **PEI-PDA** FONs. Furthermore, based on the XPS results, the percentage of DA to PEI in the **PEI-PDA** FONs is about 2.87:1, which is comparable to the experimental ratio of DA to PEI.

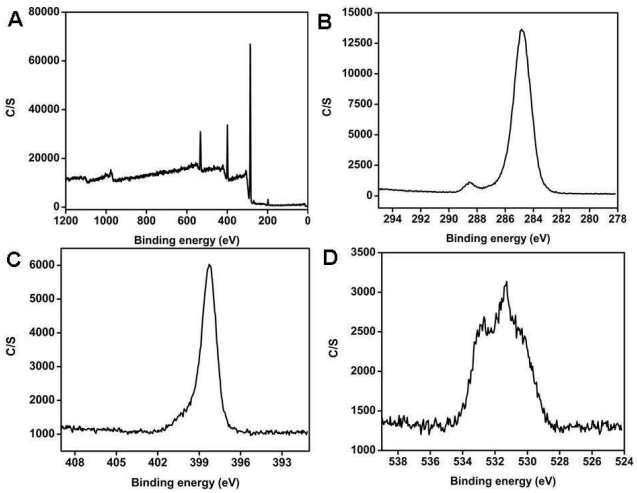


**Fig. 4** XPS spectra of PEI-PDA FONs. (A) Suvery scan of XPS spectra, (B) C1s region, (C) N1s region, (D) O1s region. The XPS spectra suggested that elements including C, N and O were existed in the sample of PEI-PDA FONs.

The photoluminescent (PL) properties of **PEI-PDA** FONs were characterized by fluorescent spectroscopy in detailed. As shown in Fig. 5, **PEI-PDA** FONs can be excited by various excitation wavelength ranged from 340-480 nm. The maxium excitation intensity of PEI-PDA FONs is located at 380 nm. When they were excited with different wavelength (340-480 nm), the emssion peak was fixed at 526 nm regardless of excitation wavelength. However, their fluorescence intensity are changed with the excitation wavelength correspondingly. The maxium fluorescence intensity can be obtained using 380 nm excitation wavelength, which is consistent with the intensity of excitation wavelength (Fig. 5). On the other hand, the effect of pH values on the fluorescent properties of **PEI-PDA** FONs was also investigated. As shown in Fig. S2. It can be seen that pH values have significant effect on the fluorescence intensity of **PEI-PDA** FONs. Relative weak fluorescence intensity can be found when **PEI-PDA** FONs dispersed in acid and alkaline solution. The maxium fluorescence intensity can be found at pH values between 7-9. These results suggested that the **PEI-PDA** FONs is stable under physiological environment, implying their biomedical potential. The fluorescent properties of **PEI-PDA** FONs is significant different from PDA FONs and carbon quantum dots in our previous reports.[43, 47, 48] In general, the emission wavelength of carbon quantum dots is dependent on the excitation wavelength. However, the emission wavelength of **PEI-PDA** FONs is not depedent on the excitation wavelength.[43, 47, 48] Due to a series of hydrophilic functional groups such as –NH, -$NH_2$ and –OH were existed in **PEI-PDA** FONs, thus obtained nanoparticles showed excellent dispersibility in aqueous solution. No perceivable aggregation was observed after they were deposited for one week (left cuvette in Fig. S3). When **PEI-PDA** FON aqueous solution was irradiated by UV lamp ($\lambda$ = 365 nm), it emitted strong green fluorescence (right cuvette in Fig. S3), which is well consistent with the photoluminscent spectra. Given the simple and scalable for preparation, high water dispersibility and strong fluorescence, the potential biological imaging applications of **PEI-PDA** FONs were further investigated.

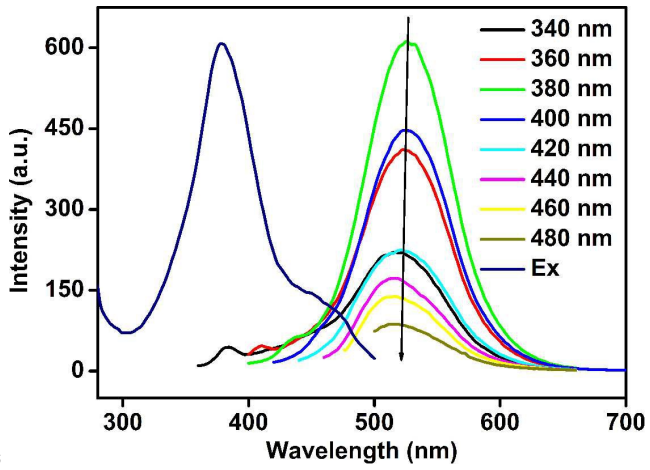


**Fig. 5** PL spectra of **PEI-PDA** FONs (in water), emission peak of **PEI-PDA** FONs is located at 526 nm, and the excitation peak is located at 380 nm. When **PEI-PDA** FONs were excited by various wavelength, fluorescent intensity of **PEI-PDA** FONs was changed correspondingly.

### 3.2 Biocompatibility evaluation of PEI-PDA FONs

Biocompatibility evaluation is very important for the biomedical applications of novel biomaterials. In this work, the biocompatibility of **PEI-PDA** FONs to A549 cells was evaluated by optical microscopy observation and cell viability measurement.[49, 50] Fig. 6A-C showed the optical images of A549 cells after they were incubated with different concentrations of **PEI-PDA** FONs for 24 h. It can be seen that cells still adhered to the cell plate very well after they were incubated with **PEI-PDA** FONs. No significant difference was found between the control cells (Fig. 6A) and **PEI-PDA** FONs treated cells (Fig. 6B and 6C). Optical microscopy observation suggested that **PEI-PDA** FONs were biocompatible with A549 cells. Furthermore, CCK-8 assay was carried out to quantitatively evaluate the effect of **PEI-PDA** FONs on A549 cells.[51, 52] As shown in Fig. 6D, almost no cell viability decrease was observed when cells were incubated with 10-120 μg $mL^{-1}$ of **PEI-PDA** FONs for 24 h. Even the concentration of **PEI-PDA** FONs is as high as 120 μg $mL^{-1}$, the cell viability values of **PEI-PDA** FONs are still greater than 91.4 ± 8.7%. Long time biocompatibility of **PEI-PDA** FONs was also evaluated after cells were incubated with **PEI-PDA** FONs for 48 h and 72 h. Results showed that the cell viability of **PEI-PDA** FONs is still greater than 92.6 ± 5.8% (Fig. S4). Furthermore, the 50% inhibition concentration (IC50) values of **PEI-PDA** FONs to A549 cells were also calculated. Our results suggested that the IC50 values of **PEI-PDA** FONs are 802.8 and 1422.9 μg $mL^{-1}$ for 48 and 72 h, respectively. The cell viability measurement further confirmed the excellent biocompatibility of **PEI-PDA** FONs. Combination of their unique fluorescence, high water dispersibility, excellent biocompatibility, and simple and scalable for preparation, thus **PEI-PDA** FONs are expected highly desirable for biomedical applications.

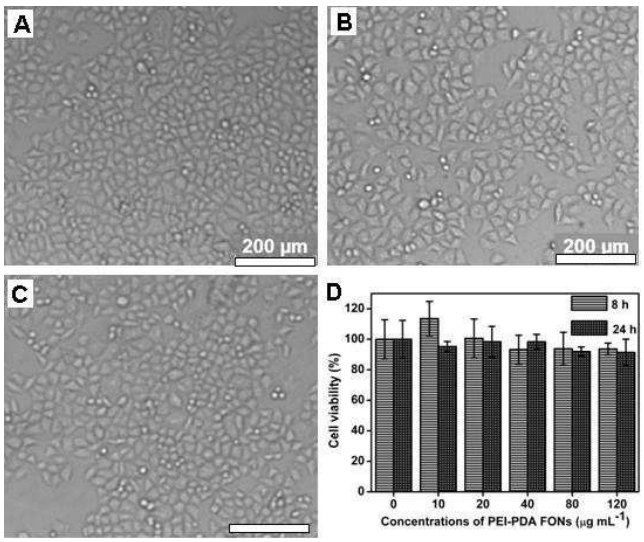


**Fig. 6** Biocompatibility evaluation of **PEI-PDA** FONs. (A-C) optical microscopy images of A549 cells incubated with different concentrations of **PEI-PDA** FONs for 24 h, (A) control cells, (B) 10 μg $mL^{-1}$, (C) 80 μg $mL^{-1}$, (D) cell viability of **PEI-PDA** FONs with A549 cells (the concentrations of **PEI-PDA** FONs are ranged from 10-120 μg $mL^{-1}$).

### 3.2 Biological imaging applications of PEI-PDA FONs

To examine the biomedical applications of **PEI-PDA** FONs, their cell uptake behavior was evaluated by CLSM.[53] As showed in Fig. 7, the cell uptake of **PEI-PDA** FONs was clearly observed after cells were incubated with 10 μg $mL^{-1}$ of **PEI-PDA** FONs for 3 h (cells were irradiated with 405 nm laser). The successful dying of cells with FONs implied the potential biological imaging applications of **PEI-PDA** FONs. It can also be found that there are many dark areas with relative weak fluorescence intensity, which were encapsulated by green fluorescence (Fig. 7B and 7C). These dark areas are possible the location of cell nucleus. As compared with the size of cell nucleus pore, size of **PEI-PDA** FONs is rather large. We therefore believed that **PEI-PDA** FONs can not enter the cell nucleus directly. More importantly, due to strong fluorescence of **PEI-PDA** FONs, the cell uptake of **PEI-PDA** FONs can be clearly observed even the concentration of FONs was as low as 10 μg $mL^{-1}$. Furthermore, if the surface of **PEI-PDA** FONs was further linked with targeting agents. The dosage used for cell imaging can be further decreased. Therefore, we believed that **PEI-PDA** FONs possess good biocompatibility for practical biological imaging applications. Due to the lack of targeting agents on the surface of **PEI-PDA** FONs, the cell imaging of **PEI-PDA** FONs should be mainly attributed to the non-specific phagocytosis.

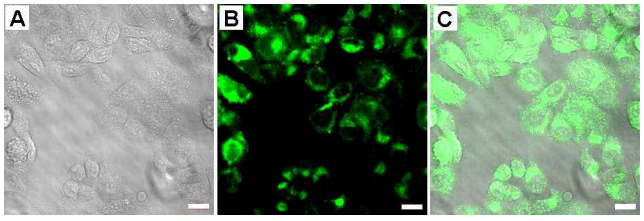


**Fig. 7** CLSM images of A549 cells when they were incubated with 10 μg $mL^{-1}$ of **PEI-PDA** FONs for 3 h. (A) bright field, (B) excited with 405 nm laser, (C) merge image of A and B. Scale bar = 20 μm.

Since the first utilization of semicondutor quantum dots for biomedical applications, a large number of fluorescent nanoprobes with different compositions have been developed.[1, 2] Among them, the fluorescent carbon nanoparticles have attracted much attention for biomedical applications for their remarkable luminescent properties, good biocompatibility, water dispersibility and low cost. Different preparation strategies and carbon sources have been reported over the past few years.[54-59] Although great advance has been made in this field, the preparation of novel fluorescent carbon nanoprobes at room temperature, air atmosphere, in aqueous solution through a green ruote with fast reaction ratio is rarely reported. As compared with previous methods, the strategy reported in this work could fulfill all of these requirements. More importantly, due to the high reactive of PDA, the novel FONs fabricated in this work can be facilely functionalized with other components through Michael addition reaction, which provide an important platform for fabrication multifunctional systems for biomedical applications.

## 4. Conclusion

In summary, **PEI-PDA** FONs were facilely prepared through self-polymerization of DA in the present of PEI for the first time. This reaction can be occured under room temperature and air atmosphere without needing catalysts and initiators, which is rather convenient, effective, green and scalable. Due to the existence of a number of functional groups such as –NH, $NH_2$ and -OH on their surface, **PEI-PDA** FONs showed excellent dispersibility in aqueous solution. On the other hand, due to the existence of reactive functional groups on the surface of **PEI-PDA** FONs, many other functional components such as drugs, targeting agents and imaging agents can be further integrated into **PEI-PDA** FONs, thus multifunctional theranostic platforms based on **PEI-PDA** FONs can be fabricated. Furthermore, PEI is a commercial available cationic polymer, which has been widely used for gene delivery. In this work, PEI was facilely incorporated into the luminescent organic nanoparticles, the **PEI-PDA** FONs are therefore may possess dual function for both biological imaging and gene delivery. Taken advantages of their easy of preparation procedure, strong fluorescence, high water dispersibility, excellent biocompatibility and multifunctional capability, **PEI-PDA** FONs should be of great research interest for various biomedical applications.

## Acknowledgements

This research was supported by the National Science Foundation of China (Nos. 21134004, 21201108, 51363016), and the National 973 Project (no. 2011CB935700)

## Notes

[a] Department of Chemistry/Institute of Polymers, Nanchang University, 999 Xuefu Avenue, Nanchang 330031, China. [b] Department of Chemistry and Key Laboratory of Bioorganic Phosphorus Chemistry & Chemical Biology (Ministry of Education), Tsinghua University, Beijing, 100084, P.

R. China. [c]Beijing National Laboratory for Molecular Sciences (BNLMS), Key Laboratory of Organic Solids, Laboratory of New Materials, Institute of Chemistry, Chinese Academy of Sciences, Beijing 100190, China.
xiaoyongzhang1980@gmail.com; weiyen@tsinghua.edu.cn

† Electronic Supplementary Information (ESI) available: Hydrodynamic size distribution and optical images of **PEI-PDA** FONs water dispersion as well as the effect of pH values on the fluorescent properties on **PEI-PDA** FONs were provided in supplementary information]. See DOI: 10.1039/b000000x/

## References


1. M. Bruchez, M. Moronne, P. Gin, S. Weiss and A. P. Alivisatos, *Science*, 1998, **281**, 2013-2016.
2. W. C. Chan and S. Nie, *Science*, 1998, **281**, 2016-2018.
3. L. Feng, C. Zhu, H. Yuan, L. Liu, F. Lv and S. Wang, *Chem. Soc. Rev.*, 2013, **42**, 6620-6633.
4. D. Ding, K. Li, B. Liu and B. Z. Tang, *Acc. Chem. Res.*, 2013, **46**, 2441-2453.
5. C. Wu, T. Schneider, M. Zeigler, J. Yu, P. G. Schiro, D. R. Burnham, J. D. McNeill and D. T. Chiu, *J. Am. Chem. Soc.*, 2010, **132**, 15410-15417.
6. F. Ye, C. Wu, Y. Jin, Y.-H. Chan, X. Zhang and D. T. Chiu, *J. Am. Chem. Soc.*, 2011, **133**, 8146-8149.
7. J. Hui, X. Zhang, Z. Zhang, S. Wang, L. Tao, Y. Wei and X. Wang, *Nanoscale*, 2012, **4**, 6967-6970.
8. X. Wang, S. Xu and W. Xu, *Nanoscale*, 2011, **3**, 4670-4675.
9. A. Shiohara, S. Prabakar, A. Faramus, C. Y. Hsu, P. S. Lai, P. T. Northcote and R. D. Tilley, *Nanoscale*, 2011, **3**, 3364-3370.
10. H. S. Choi, W. Liu, P. Misra, E. Tanaka, J. P. Zimmer, B. I. Ipe, M. G. Bawendi and J. V. Frangioni, *Nat. Biotechnol.* , 2007, **25**, 1165-1170.
11. X. Zhang, X. Zhang, B. Yang, J. Hui, M. Liu, W. Liu, Y. Chen and Y. Wei, *Polym. Chem.*, 2014, **5**, 689-693.
12. D. Ding, J. Liang, H. Shi, R. T. Kwok, M. Gao, G. Feng, Y. Yuan, B. Z. Tang and B. Liu, *J. Mater.Chem. B*, 2014, **2**, 231-238.
13. R. T. Kwok, J. Geng, J. W. Lam, E. Zhao, G. Wang, R. Zhan, B. Liu and B. Z. Tang, *J. Mater. Chem. B*, 2014, **2**, 4134-4141.
14. M. Gao, Q. Hu, G. Feng, B. Z. Tang and B. Liu, *J. Mater. Chem. B*, 2014, **2**, 3438-3442.
15. D. Ding, J. Liang, H. Shi, R. T. Kwok, M. Gao, G. Feng, Y. Yuan, B. Z. Tang and B. Liu, *J. Mater. Chem. B*, 2014, **2**, 231-238.
16. C. W. T. Leung, Y. Hong, S. Chen, E. Zhao, J. W. Lam and B. Z. Tang, *J. Am. Chem. Soc.*, 2013, **135**, 62-65.
17. H. Shi, J. Liu, J. Geng, B. Z. Tang and B. Liu, *J. Am. Chem. Soc.*, 2012, **134**, 9569-9572.
18. J. Liu, D. Ding, J. Geng and B. Liu, *Polym. Chem.*, 2012, **3**, 1567-1575.
19. Z. Wang, B. Xu, L. Zhang, J. Zhang, T. Ma, J. Zhang, X. Fu and W. Tian, *Nanoscale*, 2013, **5**, 2065-2072.
20. X. Zhang, X. Zhang, B. Yang, S. Wang, M. Liu, Y. Zhang and L. Tao, *RSC Adv.*, 2013, **3**, 9633-9636.
21. Z. Wang, S. Chen, J. W. Lam, W. Qin, R. T. Kwok, N. Xie, Q. Hu and B. Z. Tang, *J. Am. Chem. Soc.*, 2013, **135**, 8238-8245.
22. D. Ding, K. Li, B. Liu and B. Z. Tang, *Accounts Chem. Res.*, 2013, **46**, 2441-2453.
23. X. Zhang, X. Zhang, L. Tao, Z. Chi, J. Xu and Y. Wei, *J. Mater. Chemi. B*, 2014, **2**, 4398-4414.
24. Y. Liu, K. Ai and L. Lu, *Chem. Rev.*, 2014, DOI: 10.1021/cr400407a.
25. L. Zhang, J. Wu, Y. Wang, Y. Long, N. Zhao and J. Xu, *J. Am. Chem. Soc.*, 2012, **134**, 9879-9881.
26. Y. Lee, H. Lee, Y. B. Kim, J. Kim, T. Hyeon, H. Park, P. B. Messersmith and T. G. Park, *Adv. Mater.*, 2008, **20**, 4154-4157.
27. Y. Cao, X. Zhang, L. Tao, K. Li, Z. Xue, L. Feng and Y. Wei, *ACS Appl. Mater. Interfaces*, 2013, **5**, 4438–4442.
28. C. Cheng, S. Nie, S. Li, H. Peng, H. Yang, L. Ma, S. Sun and C. Zhao, *J. Mater. Chem. B*, 2013, **1**, 265-275.
29. X. Liu, J. Cao, H. Li, J. Li, Q. Jin, K. Ren and J. Ji, *ACS nano*, 2013, **7**, 9384-9395.
30. A. Postma, Y. Yan, Y. Wang, A. N. Zelikin, E. Tjipto and F. Caruso, *Chem. Mater.*, 2009, **21**, 3042-3044.
31. K. Yang, J. S. Lee, J. Kim, Y. B. Lee, H. Shin, S. H. Um, J. B. Kim, K. I. Park, H. Lee and S.-W. Cho, *Biomaterials*, 2012, **33**, 6952-6964.
32. J. Wu, L. Zhang, Y. Wang, Y. Long, H. Gao, X. Zhang, N. Zhao, Y. Cai and J. Xu, *Langmuir*, 2011, **27**, 13684-13691.
33. L. Guo, Q. Liu, G. Li, J. Shi, J. Liu, T. Wang and G. Jiang, *Nanoscale*, 2012, **4**, 5864-5867.
34. q. wan, m. liu, j. tian, F. Deng, g. zeng, z. li, K. Wang, Q. Zhang, x. zhang and y. wei, *Polym. Chem.*, 2015, 10.1039/C1034PY01565G.
35. L. Ma, H. Qin, C. Cheng, Y. Xia, C. He, C. Nie, L. Wang and C. Zhao, *J. Mater. Chem. B*, 2014, **2**, 363-375.
36. C. Cheng, S. Sun and C. Zhao, *J. Mater. Chem. B*, 2014, **2**, 7649-7672.
37. Q. Yue, M. Wang, Z. Sun, C. Wang, C. Wang, Y. Deng and D. Zhao, *J. Mater. Chem. B*, 2014, **1**, 6085-6093.
38. X. Sun, L. Cheng, J. Zhao, R. Jin, B. Sun, Y. Shi, L. Zhang, Y. Zhang and W. Cui, *J. Mater. Chem. B*, 2014, **2**, 3636-3645.
39. Y.-T. Liu, K.-C. Kung, C.-Y. Yang, T.-M. Lee and T.-S. Lui, *J. Mater. Chem. B*, 2014, **2**, 7927-7935.
40. J. Cui, Y. Wang, A. Postma, J. Hao, L. Hosta-Rigau and F. Caruso, *Adv. Funct. Mater.*, 2010, **20**, 1625-1631.
41. Y. Liu, K. Ai, J. Liu, M. Deng, Y. He and L. Lu, *Adv. Mater.*, 2013, **25**, 1353-1359.
42. K. Qu, J. Wang, J. Ren and X. Qu, *Chem. Eur. J.*, 2013, **19**, 7243-7249.
43. X. Zhang, S. Wang, L. Xu, Y. Ji, L. Feng, L. Tao, S. Li and Y. Wei, *Nanoscale*, 2012, **4**, 5581-5584.
44. X. Zhang, H. Qi, S. Wang, L. Feng, Y. Ji, L. Tao, S. Li and Y. Wei, *Toxicol. Res.*, 2012, **1**, 201-205.
45. X. Zhang, J. Ji, X. Zhang, B. Yang, M. Liu, W. Liu, L. Tao, Y. Chen and Y. Wei, *RSC Adv.*, 2013, **3**, 21817-21823.
46. X. Zhang, M. Liu, Y. Zhang, B. Yang, Y. Ji, L. Feng, L. Tao, S. Li and Y. Wei, *RSC Adv.*, 2012, **2**, 12153-12155.
47. X. Zhang, S. Wang, C. Zhu, M. Liu, Y. Ji, L. Feng, L. Tao and Y. Wei, *J. Colloid Interf. Sci.*, 2013, **397**, 39-44.
48. X. Zhang, S. Wang, M. Liu, B. Yang, L. Feng, Y. Ji, L. Tao and Y. Wei, *Phys. Chem. Chem. Phys.*, 2013, **15**, 19013-19018.
49. Q. Wei, F. Zhang, J. Li, B. Li and C. Zhao, *Polym. Chem.*, 2010, **1**, 1430-1433.
50. X. Zhang, J. Yin, C. Peng, W. Hu, Z. Zhu, W. Li, C. Fan and Q. Huang, *Carbon*, 2011, **49**, 986-995.
51. X. Zhang, W. Hu, J. Li, L. Tao and Y. Wei, *Toxicol. Res.*, 2012, **1**, 62-68.
52. X. Zhang, S. Wang, M. Liu, J. Hui, B. Yang, L. Tao and Y. Wei, *Toxicol. Res.*, 2013, **2**, 335-346.
53. B. Yang, Y. Zhang, X. Zhang, L. Tao, S. Li and Y. Wei, *Polym. Chem.*, 2012, **3**, 3235-3238.
54. X. Wang, K. Qu, B. Xu, J. Ren and X. Qu, *J. Mater. Chem.*, 2011, **21**, 2445-2450.
55. L. Zhou, Y. Lin, Z. Huang, J. Ren and X. Qu, *Chem. Commun.*, 2012, **48**, 1147-1149.
56. X. Ran, H. Sun, F. Pu, J. Ren and X. Qu, *Chem. Commun.*, 2013, 49, 1079-1081.
57. H. Sun, L. Wu, N. Gao, J. Ren and X. Qu, ACS Appl. Mater. Interfaces, 2013, 5, 1174-1179.
58. B. De and N. Karak, RSC Adv., 2013, 3, 8286-8290.
59. K. M. Tripathi, A. K. Sonker, S. K. Sonkar and S. Sarkar, RSC Adv., 2014, 4, 30100-30107.

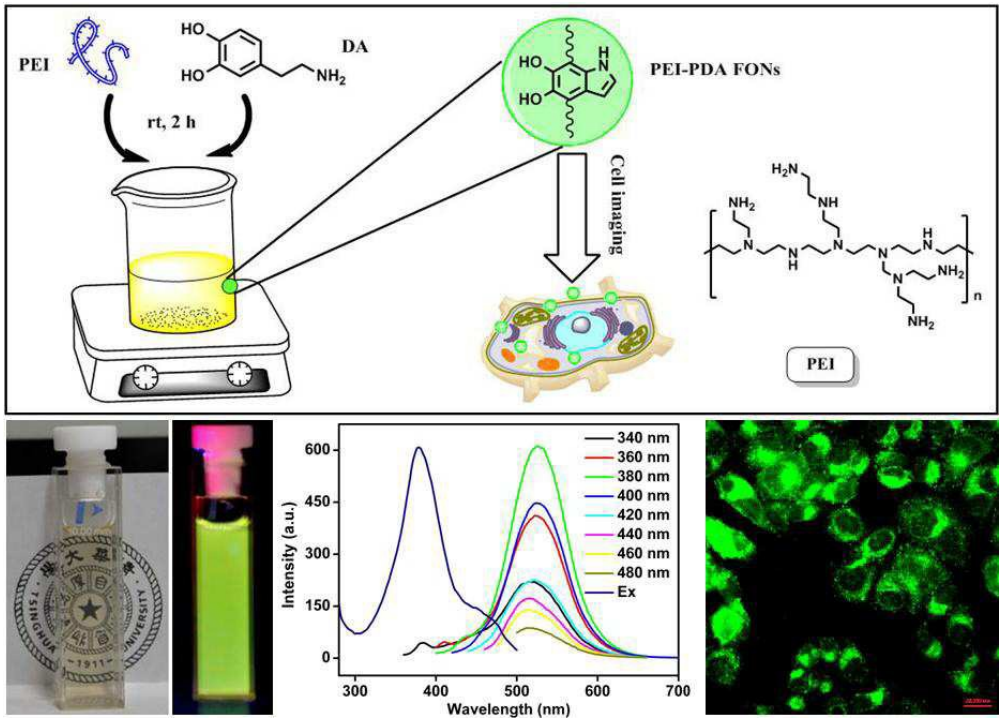


Novel fluorescent organic nanoparticles based on self-polymerization of dopamine and Polyethyleneimine were prepared and utilized for biological imaging applications